2016-12

Slip-partitioned surface ruptures for the Mw 7.0 16 April 2016 Kumamoto, Japan, earthquake

Toda, S

10.1186/s40623-016-0560-8
Earth Planets and Space
Terra Scientific Publishing Company

Toda *et al. Earth, Planets and Space* (2016) 68:188
DOI 10.1186/s40623-016-0560-8

Earth, Planets and Space

FRONTIER LETTER

Open Access

Slip-partitioned surface ruptures for the Mw 7.0 16 April 2016 Kumamoto, Japan, earthquake

Shinji Toda[1*], Heitaro Kaneda[2], Shinsuke Okada[1], Daisuke Ishimura[3] and Zoë K. Mildon[4]

Abstract

An ENE-trending ~30-km-long surface rupture emerged during the Mw = 7.0 16 April 2016 Kumamoto earthquake along the previously mapped Futagawa and northern Hinagu faults. This included a previously unknown 5-km-long fault within the Aso Caldera, central Kyushu. The rupture zone is mostly composed of right-lateral slip sections, with a maximum of 2-m coseismic slip. One of the noteworthy features we observed in the field are ~10-km-long segmented normal fault scarps, dipping to the northwest, along the previously mapped Idenokuchi fault, 1.2–2.0 km south of and subparallel to the Futagawa fault. The maximum amount of coseismic throw on the Idenokuchi fault is ~2 m, which is nearly equivalent to the maximum slip on the strike-slip rupture. The locations and slip motions of the 2016 rupture are also manifested as interferogram fringe offsets in InSAR images. Together with geodetic and seismic inversions of subsurface fault slip, we present a schematic structural model where oblique motion occurred on a northwest-dipping subsurface fault and the slip is partitioned at the surface into strike-slip and normal fault scarps. Our simple dislocation model demonstrates that this bifurcation into pure strike-slip and normal faults likely occurs for optimally oriented failure near the surface. The Kumamoto case, with detailed geological observations and geophysical models, would be the second significant slip-partitioned earthquake around the globe. It provides an important insight into scale- and depth-dependent stress heterogeneity and an implication to a proper estimate of seismic hazard in complex and broad multiple fault strands.

Keywords: 2016 Kumamoto earthquake, Surface rupture, Slip partitioning, Active fault

Introduction

The 16 April 2016 Mw = 7.0 (Mjma = 7.3) Kumamoto earthquake struck the cities of Kumamoto, Mashiki, Nishihara and Minami-Aso from the Kumamoto plain to the western edge of Aso Caldera in central Kyushu, and brought significant damage to buildings, killing 50 people (Fig. 1). The 16 April earthquake ruptured a northern part of the Hinagu fault and the Futagawa fault and extended northeast to a previously unknown 5-km-long NE-trending strike-slip fault within the Aso Caldera. The hypocenter is located ~5 km west from the junction of the Futagawa and Hinagu faults, where the 14 April 2016 Mw = 6.2 (Mjma = 6.5) earthquake was preceded on the Hinagu fault zone, 2.5 km south of the fault junction (Fig. 1). In this paper, we define the Kiyama fault, Futagawa fault and Kitamukaiyama fault previously mapped in Research Group for Active Faults of Japan (1991) as our Futagawa fault for simplicity. Even though possible minor cracks at a few isolated locations were reported on the Hinagu fault, this foreshock produced no discernible surface effects.

The sequence of the 2016 Kumamoto earthquakes occurred in the center of Kyushu Island where N–S stretching has been ongoing since 6 Ma (Kamata and Kodama 1994). Subduction-related volcanism started at ~1.5 Ma in Kyushu (Kamata et al. 1988) and has been significantly promoted by the rift-zone activity along the Beppu-Shimabara Rift Zone (BSRZ, Matsumoto 1979). The BSRZ is composed of numerous EW-trending

*Correspondence: toda@irides.tohoku.ac.jp
[1] International Research Institute of Disaster Science, Tohoku University, Aoba, 468-1, Aoba, Sendai 980-0845, Japan
Full list of author information is available at the end of the article

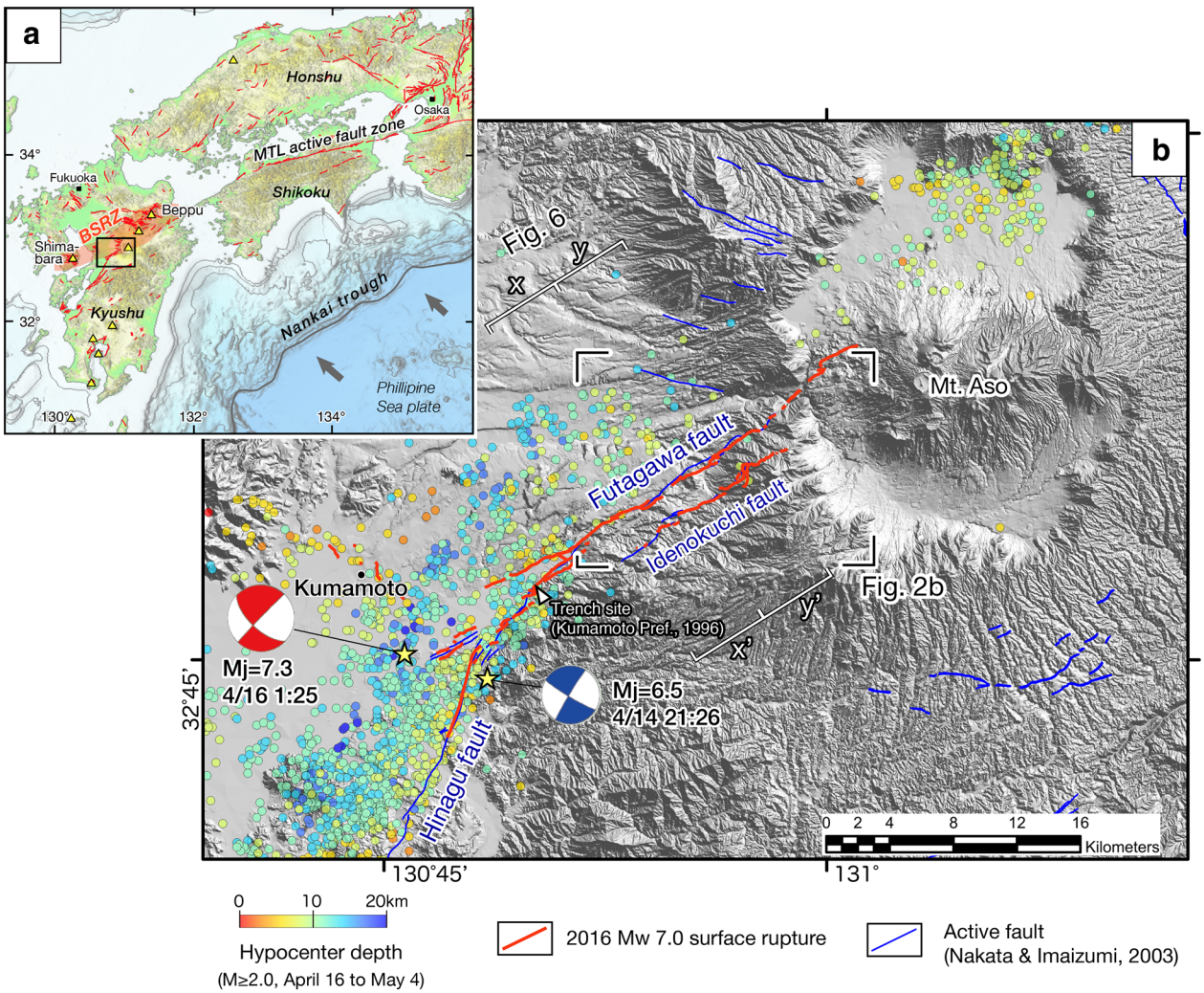

Fig. 1 Locations of the surface ruptures associated with the 2016 Kumamoto earthquake. **a** Map showing the tectonic setting, active volcanoes and active faults in southwest Japan. Active faults are shown with *red lines* (Research Group for Active Faults of Japan, 1991). The source area of the 2016 Kumamoto earthquake shown in **b** is enclosed with a *black rectangle* at the center of Kyushu Island. **b** Map of the 16 April 2016 surface rupture (Kumahara et al. 2016). Previously mapped active faults are shown as *blue lines*. Focal mechanisms of both Mjma = 6.5 14 April and Mjma = 7.3 16 April are shown with their epicenters (*yellow stars*), together with aftershocks since the Mjma = 7.3 event

normal faults synchronous with extensive volcanism. Right-lateral motion along the southern margin of the BSRZ, also known as the Oita-Kumamoto Tectonic Line (Yabe 1925), is thought to have been active since 0.5 Ma following the onset of dextral motion of the Median Tectonic Line in Shikoku Island (Fig. 1a) since 2 Ma (Tsukuda 1990), involving several caldera-forming eruptions. The Aso Caldera, a part of the 2016 rupture zone, was formed by four major catastrophic eruptions from ~270 to 90 ka (Ono and Watanabe 1985). Present-day N–S extension occurs at a rate of 1–2 cm/year across the BSRZ, detected by both decadal triangulation networks (Tada 1984) and modern GPS networks (e.g., Nishimura and Hashimoto 2006), together with frequent small-to-moderate magnitude normal faulting earthquakes. The Futagawa fault, striking N60°E, forms part of the Oita-Kumamoto Tectonic Line and was a predominant part of the 2016 seismic source. The fault has been accommodating N–S stretching on the southern margin of the BSRZ. This fault is hypothesized to be a right-lateral strike-slip fault with significant southeast-side-up vertical movement, making an E–W-trending graben and contributing to the subsidence of the Kumamoto Plain (e.g., Ishizaka et al. 1995). In contrast the ~80-km-long and N40°E-trending Hinagu fault, located outside the BSRZ, is more favorably oriented for right-lateral strike-slip faulting, except the

central and southern sections that are estimated to have modest east-side-up vertical movement (Research Group for Active Faults of Japan 1991).

Such differences in geometry and stress field between the Hinagu fault and Futagawa fault are manifested as the different surface rupture traces and slip senses associated with the Mw = 7.0 16 April Kumamoto earthquake. Our field observations revealed that a ~10-km stretch of the 20-km-long Futagawa fault rupture was accompanied by a series of normal fault scarps along the previously mapped Idenokuchi fault (Fig. 1b). Together with a NW-dipping source fault inferred from the aftershock distribution and geodetic inversion, we found that the slip-partitioned fault breaks occurred during the Kumamoto earthquake. This could be the second significant case of coseismic slip partitioning after the 2001 Kokoxili, China, earthquake (King et al. 2005) and gives us a great opportunity to understand the mechanism of the slip partitioning and to gain clues for rupture dynamics and long-term fault development in a complex stress environment. In this paper, we describe the significant features of coexistence of strike-slip and normal faulting ruptures associated with the 2016 Kumamoto earthquake and then illustrate a possible mechanism of such a slip partitioning and its implication to seismic hazard evaluation.

The 2016 earthquake surface rupture

Detailed mapping of the surface break and measurements of fault offsets were undertaken from 16 April to 16 June by ~20 research scientists from numerous Japanese universities. The mapping observations, coordinated by Associate Prof. Kumahara (Kumahara et al. 2016), conclude that the surface rupture associated with the 16 April 2016 event is ~30 km long, involving 6 km of the northernmost part of the Hinagu fault with up to ~0.6-m right-lateral slip, and a 20-km-long break on the Futagawa fault with up to ~2.0-m right-lateral slip. The rupture progressed easterly for another 5 km on an unknown right-lateral strike-slip fault into the Aso Caldera with up to 1-m right-lateral slip. A series of left-stepping en-echelon fractures, corresponding to right-lateral faulting, from meter to kilometer scale are visible in the field and along mapped surface rupture traces. On a large scale, these ground breaks mostly follow the previously mapped active fault traces of the Hinagu and Futagawa fault zones identified as significant faulted landforms (e.g., Research Group for Active Faults of Japan 1991; Nakata and Imaizumi 2002) (Fig. 1). However, on a small scale, there are numerous small fault branches, parallel-running rupture traces, and short conjugate NW-trending left-lateral faults occurring off the mapped faults, demonstrating complex surface phenomena.

Slip partitioning at the 2016 earthquake

During the surface rupture mapping project, the authors of this paper were mostly in charge of the eastern portion of the Futagawa fault, where we found a 10-km stretch of coexistent coseismic normal and right-lateral strike-slip ground breaks separated by up to 2 km.

Right-lateral strike-slip fault zone

In the slip-partitioned zone of surface ruptures, several left-stepping segments (each on the order of a few kilometers long) characterize the strike-slip surface rupture (Fig. 2). Each fault trace is straight on a map, suggesting that the fault dip near the surface is almost vertical. One section bisects the Omine volcanic cone at 4–5 km horizontal distance in Fig. 2; this is one of the parasitic eruption centers out of the Aso Caldera that last erupted ~0.1 Ma (Watanabe et al. 1979). The entire section of the strike-slip rupture zone can be divided into two subsections. Fault traces west of the Omine volcanic cone follow older fault scarps along which we observed several local normal faulting ruptures that might have amplified the height of the preexisting scarps. East of Omine volcanic cone the fault traces cut the outer rim of the caldera and do not show any significant vertical separation during the Kumamoto earthquake.

We measured both lateral and vertical offsets of man-made features such as paved roads, dirt roads, and rice paddy dikes. In our study area along the eastern Futagawa fault, the largest right-lateral slip was 1.65 m, and this was observed at 7 km mark along the section (Figs. 3, 4b). In contrast, displacements west of the Omine volcano, from 0- to 3-km mark, are significantly smaller (0.1–0.3 m). Slip also tapers toward Aso Caldera to the east, being about half of the maximum slip. The average slip over the fault zone is ~0.7 m. The most prominent feature of the strike-slip section is that the movement is purely right-lateral. Although measurable vertical movements less than 30 cm were observed at several locations, up-thrown and down-thrown sides frequently switch along the rupture zone. We thus hypothesize that these are local tectonic features and/or small-scale topographic effects.

Normal faulting rupture zone

A normal surface rupture zone ~10 km in length predominantly emerged along the previously mapped 7-km-long Idenokuchi fault (Research Group for Active Tectonics in Kyushu 1989, Fig. 1). The overall vertical slip sense is southeast-up, which is consistent with the large-scale topography as shown in Fig. 2. The trend of the normal fault zone is N55°E, parallel to the trend of the strike-slip fault zone. The separation distance between

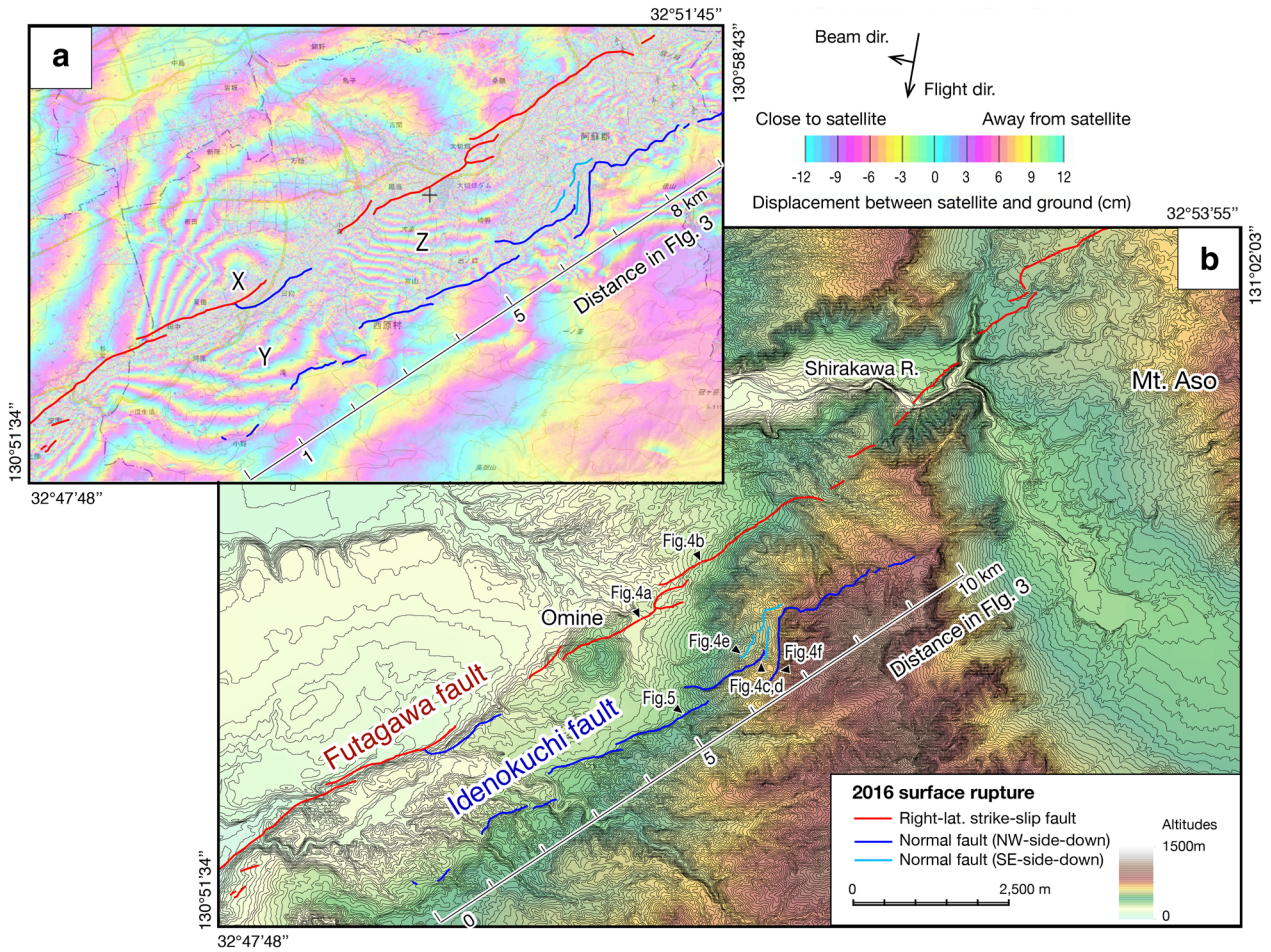

Fig. 2 Distribution of fresh normal fault scarps subparallel to the right-lateral slip surface breaks in the eastern part of the 2016 rupture zone. **a** Map showing spatial relation between observed ground breaks and descending interferograms computed from ALOS-2/PALSAR-2 images of 7 March 2016 and 18 April 2016 (Geospatial Information Authority of Japan 2016a). Marks X, Y and Z are reference locations for descriptions in text. **b** Detailed rupture distribution of the eastern half of the 2016 ground break zone, superimposed on the altitude tints and topographic contours (20-m interval). Locations of the photographs in Figs. 4 and 5 are marked

the two zones is 1.2–2.0 km. The normal rupture zone is comprised of several left-stepping sections and significant fault bend where the strike differs by ~50° from the overall trend of the fault zone.

A predominant morphological style of the surface rupture was a near-vertical free face of thick unconsolidated sediments and/or soil units involving a tensile (opening) component of up to ~1 m and occasionally with a colluvial wedge present. Tilted trees and meter-scale local landslides triggered by fault slip were commonly observed along the rupture zone. Since most of the surface breaks are located on steep slopes in the deep forest and ranches (Fig. 4), we measured vertical offsets using a measuring tape, folding ruler, leveling staff and/or hand-level, which includes approximately ±10-cm measurement errors. At key locations, we measured vertical separation by taking surface profile using a laser distance meter (Laser Technology TruPulse 200X) and a target prism that gives a measurement accuracy of ±4 cm. There were few observations of man-made features as piercing points, and hence, we could not measure the amount of slip more accurately, in particular lateral slip. The maximum vertical slip of ~2.0 m was measured at a 6.7-km mark (Fig. 3), gradually tapering toward the west and east (Fig. 3b). But it is comprised of several triangle slip distributions corresponding to several subsections. The throw averages 0.7 m, approximately equivalent to the average right-lateral slip in the strike-slip zone.

We note two minor features in the coseismic surface ruptures along the normal fault zone. One is left-lateral slip of up to 1.2 m accompanying the normal faulting (Fig. 3b). These left-lateral features were discernible from

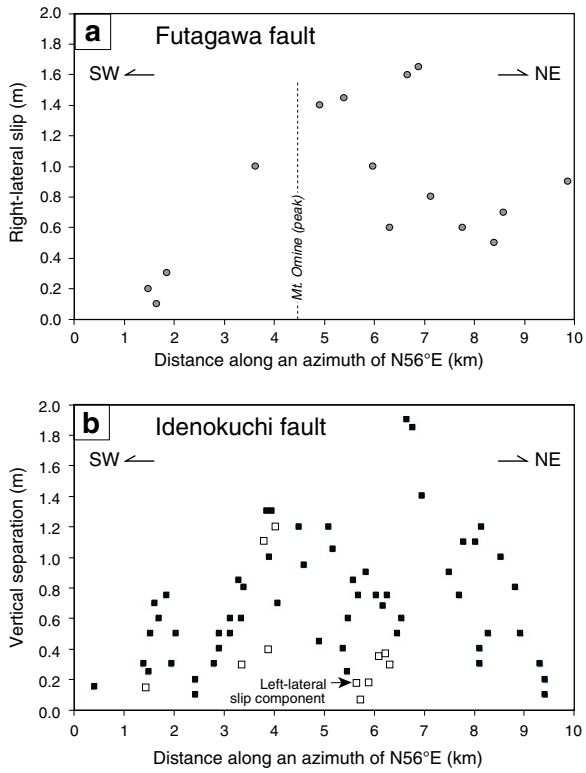

Fig. 3 Slip distribution of the 2016 rupture on the eastern section of the Futagawa fault (**a**) and the Idenokuchi fault (**b**). Discernible left-lateral slip component on normal slip, not pure left-lateral slip, is also plotted as open square in **b**. The distance along strike scale is shown in Fig. 2

man-made features and by jigsaw matching and the restoration of detailed rupture shapes between the up-thrown side and down-thrown side. The other observed feature is an antithetic fault that locally uplifts the downslope side of the main fault zone making the uphill-facing fresh scarp (Fig. 4e). A significant antithetic (south-dipping) rupture scarp at 6.2- to 7.3-km mark emerged exactly along the northern foothill of tectonic geomorphic bulges (pale blue lines in Fig. 2b). These two minor but important features enable us to prove that these 10-km-long continuous scarps are purely tectonic, not a product of a massive landslide or a combination of local landslides.

At several places, a fresh fault surface was preserved on the scarp face, a fault dip being ~60° to ~70° northwest. At one location, we found a fault scarp on a mountain slope, beneath which a waterway tunnel is also vertically deformed by ~1.0 m, providing a rare opportunity to evaluate near-surface fault dip (Fig. 5a). Laser distance meter profiling of the ground surface as well as the bed of the waterway tunnel suggests that a fault dip of 60° best explains locations of fault scarp and waterway deformation (Fig. 5b).

Fault locations on InSAR image

Synthetic aperture radar (SAR) images were obtained by the ALOS-2/PALSAR-2 and were analyzed by Geospatial Information Authority of Japan (2016a). These images reveal that there is an E–W elongated crustal block sandwiched between the strike-slip and normal faulting traces and it moved separately from the surrounding crust. The locations of the interferogram fringe offsets are consistent with the positions of the strike-slip and normal faulting zones we found in the field (Fig. 2a).

A set of concentric semicircular fringes north of the strike-slip zone indicate a broad zone of subsidence centered 1.5 km along the studied rupture zone (X in Fig. 2a). Another concentric semicircle marked as Y in Fig. 2a appears in the western part of the normal fault zone, also suggesting subsidence in this region. Since the fringe patterns and fringe intervals of point Y differ from the ones south of the normal fault zone, we hypothesize that there is a subsurface continuous normal fault in this area with intermittent short surface breaks (mark 0–3 km in Fig. 2a). Dense E–W-striking fringes at the central portion (mark 3–6 km, Z in Fig. 2a) indicate significant subsidence bounded by the normal fault zone. There are 12 fringes present, suggesting approximately 1.5 m increase in range (further away from the satellite), corresponding to subsidence. There are several discrete fringes south of the normal fault zone, which might be related to other short tectonic breaks, but we have not yet confirmed this in the field. Despite poor coherence, the other third of the slip-partitioned block at mark 6–9 km (Fig. 2a) is also shown as densely distributed fringes clearly separated from the surrounding crust.

These remarkable several kilometer-scale features are omitted in the geodetic inversion model that assigns slip and rake on subfault patches of a single rectangular fault plane (Geospatial Information Authority of Japan 2016a).

Discussion

Schematic illustration

Our interpretation from the field observations detailed in this paper indicates that the vertical strike-slip Futagawa fault and the ~60° north-dipping Idenokuchi normal fault which are separated by ~2 km at the surface intersect at a depth of 3.5 km. The overall slip distribution profiles along the strike-slip and normal fault strands are similar both in shape and in amount (Fig. 3), suggesting that movements on these two faults are intimately linked and share a common origin. We thus infer that the two faults are upward bifurcations from a deeper north-dipping source fault at seismogenic depths. Despite large scattering and a paucity of aftershocks, a seismic cross section indicates that the subsurface fault dips 50°–70° northwest (Fig. 6), consistent with the InSAR analysis (Geospatial

Fig. 4 Photographs of features of the 2016 Kumamoto earthquake surface rupture. **a** Displaced centerline of the paved road next to the Okiribata dam. *Arrows point* along fault trace. **b** Pure right-lateral slip of the concrete road. *Arrows point* along fault trace. **c** Normal fault scarp cut a grass slope in a ranch. Coseismic vertical separation at the site is ~1 m, but the cumulative topographic offset is evident. **d** Free face of the unconsolidated soil and volcanic ash unit on a normal fault scarp in the grass slope. **e** Uphill-facing normal fault scarp on a grass slope. It is interpreted as an antithetic fault. **f** Maximum ~2.0-m vertical separation of a forestry road

Information Authority of Japan 2016a). A variable slip model inverted from seismic waveforms also displays a remarkable oblique motion on a north-dipping fault along the eastern Futagawa fault (Kubo et al. 2016). We illustrate in Fig. 7 a schematic structural model for slip during the earthquake.

We thus conclude that slip partitioning occurred during the 2016 Kumamoto earthquake. The term "slip partitioning" is used to describe oblique motion along a fault system that is accommodated on two or more faults with different mechanisms (Fitch 1972; McCaffrey 1992; Jones and Wesnousky 1992; Bowman et al. 2003). Slip

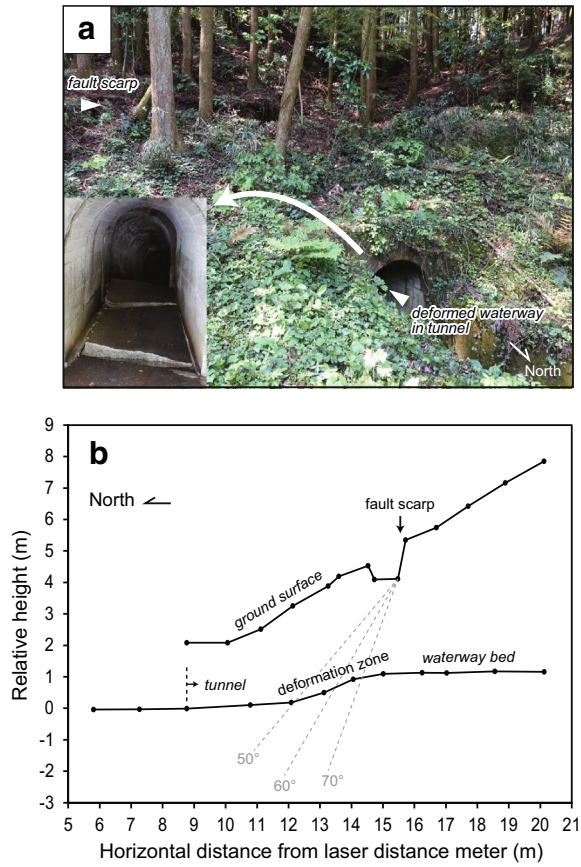

Fig. 5 A better estimate of a near-surface fault dip from a combination of surface profiling and waterway tunnel deformation. **a** Photograph of a fault scarp on a mountain slope, beneath which the waterway tunnel is deformed. *Inset* shows a photograph of the deformed waterway bed in the tunnel. **b** Profiles of the ground surface and waterway bed based on a laser distance meter survey. *Dashed gray lines* indicate possible surface fault dips, and a dip of 60° best fits the location of the fault scarp and the deformation zone

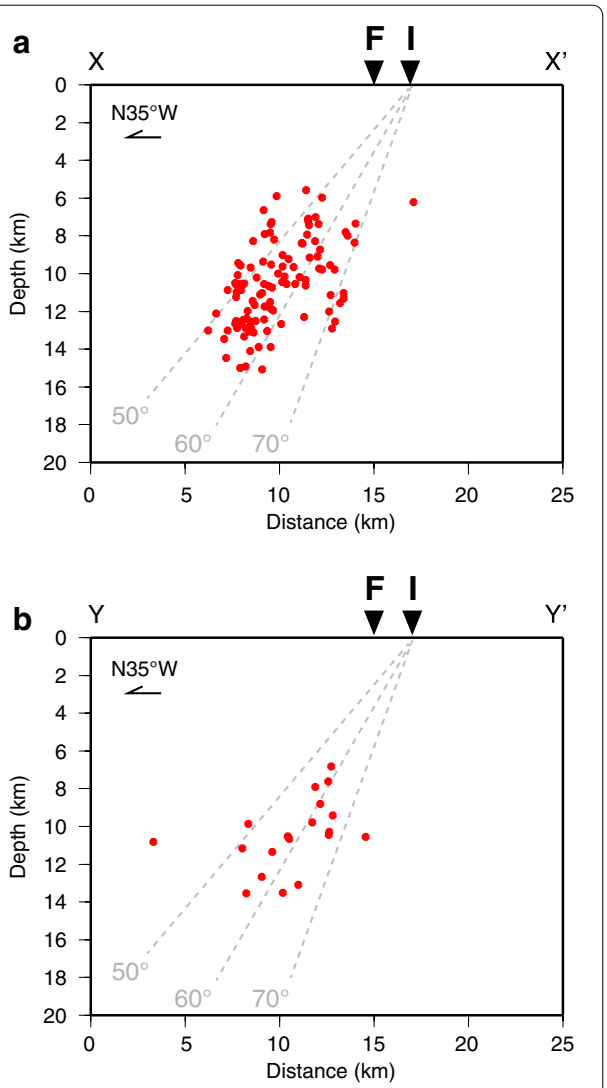

Fig. 6 Seismic cross sections of the aftershocks across the Futagawa (F) and Idenokuchi (I) fault zones. Locations are from the temporal JMA catalog downloaded on 27 June 2016. The locations of the 5-kilometer-wide strips of x–x′ and y–y′ are shown in Fig. 1

partitioning is observed at a variety of scales. For example, Fitch (1972) observed that larger-scale (over 100 km) slip partitioning occurs along subduction systems. As shown in Fig. 1a, an oblique subduction of the Philippine Sea plate underneath southwest Japan is accommodated not only by the megathrust earthquakes along the Nankai Trough but also by right-lateral slip along the Median Tectonic Line (MTL) active fault system. The separation distance between the Nankai Trough and the MTL is over 100 km, which is comparable with depth of the upper mantle and the thickness of the plate. Partitioned slip separated by several tens of kilometer distance was explained by deeper oblique driving motion in viscous lower crust (Bowman et al. 2003). Slip partitioning could be explained as a result of upward propagation of oblique shear at depth. The authors validated the model by applying it to parts of the San Andreas and Haiyuan faults.

Nevertheless, neither plate scale nor entire crustal scale movement would cause slip partitioning to occur for a single earthquake, even though slip partitioning at several kilometer scale has been documented elsewhere. Simultaneous movements of strike-slip and dip-slip faults at a single earthquake were first observed at the Mw 7.8 2001 Kokoxili earthquake along the Kunlun fault (King et al. 2005). These authors adopted Bowman's idea to the Kokoxili earthquake and then concluded that slip partitioning is a consequence of rupture propagation within the brittle upper crust, and thus, it would not occur if all parts of a fault move simultaneously. The 2016 Kumamoto earthquake would be the second significant case among well-observed recent earthquakes.

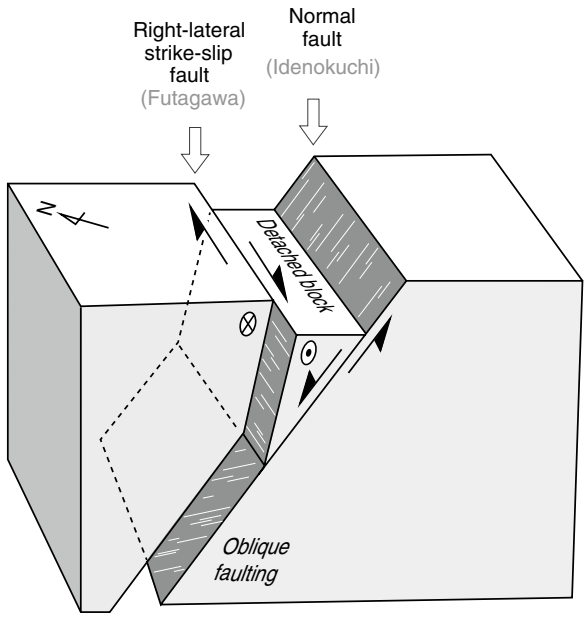

Fig. 7 Schematic illustration of slip partitioning from depth to the surface that occurred during the 2016 Kumamoto earthquake. The planes of movement are shown in *dark gray*, and the *white lines* in these areas indicate the slip direction

Dislocation model

We here demonstrate a simple mechanical model of faulting in elastic half-space from Okada (1992) with several constraints from field observations and estimated fault dip at depth. We followed the fundamental hypothesis of the mechanics of slip partitioning proposed by Bowman et al. (2003) and King et al. (2005) which models movement on a buried oblique fault and the deformation field near the surface is analyzed.

In the elastic half-space with Poisson's ratio of 0.25 and Young's modulus of 8.0×10^5 bar, an oblique buried fault is modeled. The fault strikes 235° and dips 60°N, the top and bottom depths of the fault are 3.5 and 12 km, respectively, and 1.5-m right-lateral slip and 1.5-m normal slip are assigned. We then calculated shear stress change for a pure right-lateral strike-slip fault (Fig. 8a) and for a pure normal fault (Fig. 8b). As a result, near the surface, we found the maximum shear stress for strike-slip receiver faults is located exactly above the upper termination of the oblique fault, whereas the one for a normal fault is positioned at the up-dip extension. These positions coincide with the locations of the mapped strike-slip and normal faulting rupture zones. Thus, our demonstration supports the idea that the rupture propagated upward from depth to near the surface where the final deformation occurred (Bowman et al. 2003; King et al. 2005). Our advantage to understand the slip partitioning at the 2016 Kumamoto earthquake is a well-constrained source fault geometry that could not be proven in the 2001 Kokoxili earthquake (King et al. 2005).

An additional minor feature of the Kumamoto slip partitioning is a small amount of left-lateral slip on the normal fault (Fig. 3b). Here we also examined the shear stress change for a left-lateral fault parallel to the NE-striking source fault in the dislocation model (Fig. 8c). We found that the driving stress from the buried oblique fault inhibits left-lateral slip on the NE-trending normal fault. However, if right-lateral faulting had occurred immediately before the normal faulting, it would have added moderate left-lateral shear stress on the normal fault. Our simple calculation may suggest that the right-lateral movement occurred first, followed by normal faulting during the coseismic process, in addition to the upward propagation of the rupture. It should be noted that the effects of dynamic rupture propagation differ from those in a static model.

Perpetual features (topographic expression)

It is unclear whether corupture of the strike-slip fault and normal fault occurred solely during the 2016 event, or whether slip partitioning would always be a feature of the rupture of the source fault at depth. Normal faulting has occurred along the previously mapped ~7-km-long Idenokuchi fault that displaces the 90-ka pyroclastic deposits by up to 60 m (Research Group for Active Tectonics in Kyushu 1989), yielding a slip rate of 0.7 mm/year. In the field, we observed cumulative vertical separation of the NW-facing slope (Fig. 4c). The long-term right-lateral strike-slip rate along the Futagawa fault section is poorly known due to the difficulty in estimating ages of piercing points. At one location, a paleoseismic trench excavation (Fig. 1b) immediately southwest of our study area in Mashiki Town provides a right-lateral strike-slip rate of 0.25 mm/year (Kumamoto Prefecture 1996), which is one-third of the normal faulting rate on the Idenokuchi fault. However, the right-lateral strike-slip around this trench site was only ~0.5 m in 2016 (Kumahara et al. 2016), as compared to the maximum right-lateral strike-slip of ~2 m to the northeast. This implies that the maximum slip rate of the strike-slip fault is substantially larger than the estimate at this trench. We therefore suggest that slip rates of strike-slip and normal faulting are roughly equivalent, which would be consistent with the amounts of slip observed at the 2016 event. We thus believe that these near-surface tectonic structures are long-lived features, and coseismic slip partitioning behavior has frequently occurred in the past, in particular since the last caldera-forming eruption.

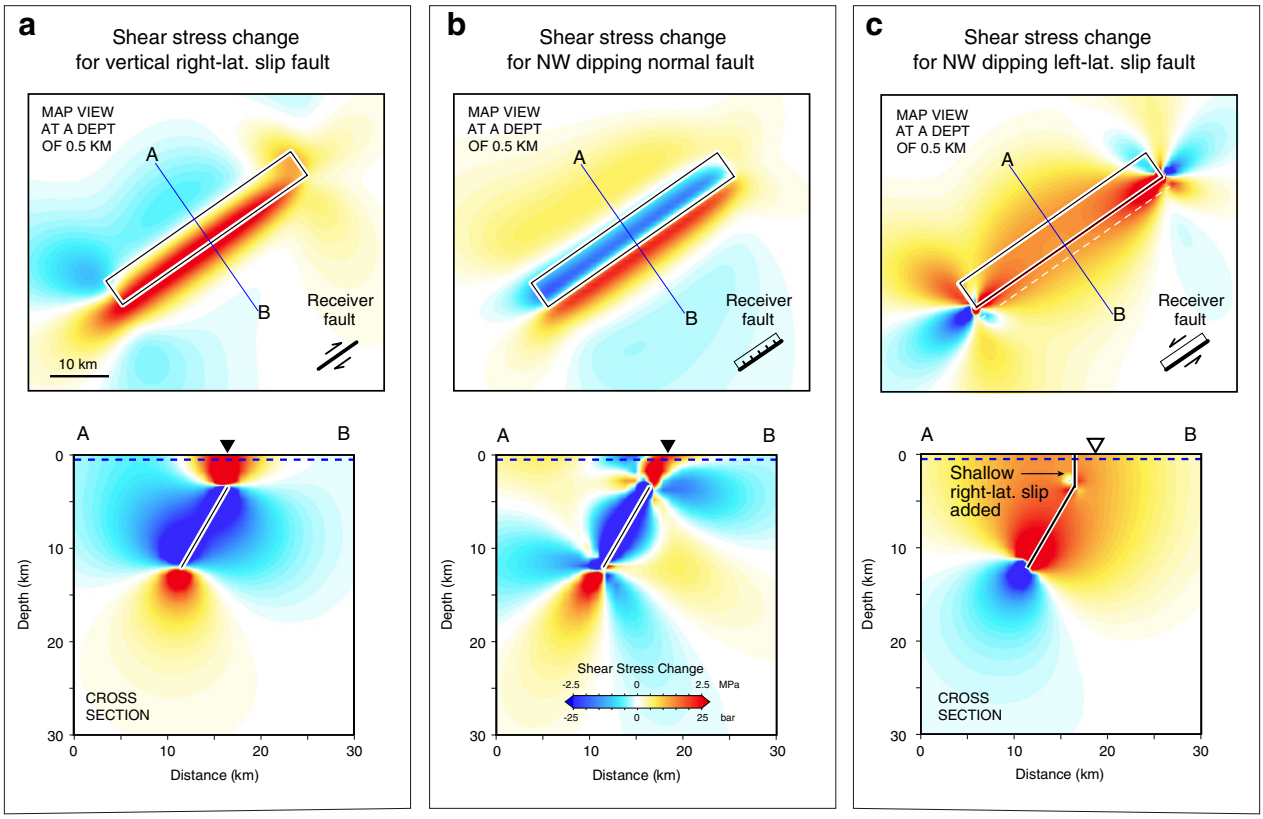

Fig. 8 Simple dislocation models to explain the slip partitioning. **a** Shear stress change for a right-lateral strike-slip fault caused by an oblique slip at depth, **b** shear stress change for a normal fault caused by an oblique slip at depth and **c** shear stress change for left-lateral strike-slip movement on NW-dipping fault due to a combination of blind oblique slip and surface right-lateral slip. High stress shown in the models supports the partitioning of the slip on the different faults near the surface and possibly suggests that the right-lateral slip occurred before the normal slip

Location of asperity, aftershock productivity and postseismic deformation

It is interesting to note that location of a large asperity with up to 5-m net slip from the seismic waveform inversion (Kubo et al. 2016) corresponds to the section of slip partitioning. The variable slip model may also explain the paucity of aftershocks on this slip-partitioned section (Figs. 1, 6) if the large slip released accumulated strain and generated a stress shadow. But we propose another reason for the lack of aftershocks. A significant normal fault slip relative to the western part of the 2016 rupture zone (out of our study area) might have strengthened the fault zone, according to a model suggested by Sibson (1992). Figure 2 in Sibson (1992) illustrates that both normal stress and frictional strength decrease through the interseismic period on an optimally oriented normal fault due to a reduction of horizontal stress, and frictional strength suddenly increases immediately after failure.

Another intriguing feature that might be related to the slip partitioning is that a minor postseismic subsidence of a few centimeters occurred in the crustal block bounded by the Futagawa and Idenokuchi faults. It was clearly detected by interferograms of ALOS-2/PALSAR-2 data using a pair of SAR images obtained on 17 April 2016 and 2 May 2016 (Geospatial Information Authority of Japan 2016b). We hypothesize that this faint subsidence occurred in the partially detached block from the surrounding crust (Fig. 7).

Implication to the stress field estimate and seismic hazard analyses

Coseismic slip partitioning during the Kumamoto earthquake provides us with a caveat against stress tensor inversion (e.g., Michael 1984) using local geological data. It could be argued that the coordinates of the principal stress axes near the Idenokuchi fault, which are favorable for normal faulting, are different from the ones along the Futagawa fault. But it could also be deduced that a large group of samples from the 2016 rupture zone would reproduce a representative stress field along the southern

BSRZ with a mix of two types of fault slip. It demonstrates a good example of scale and depth dependency of the stress heterogeneity (e.g., Smith and Heaton 2011) and sample size dependency in space and time in the stress tensor inversion.

On the other hand, the Kumamoto earthquake furnishes an important clue to properly evaluate grouping multiple fault strands. Coexistence of different type faults within several kilometers, narrower than seismogenic source dimensions, does not exclude them being individual seismic sources. Instead, multiple fault strands, even different slip sense, may be joined together as a single seismogenic source at depth. For example, the Median Tectonic Line active fault system in Shikoku Island is comprised of a dipping strike-slip fault system involving secondary parallel thrust fault traces. This could be a candidate to investigate the hypothesis further. The Kumamoto earthquake, for which the Futagawa and Idenokuchi faults were previously identified, would have been such a case. This case fits the limiting dimension of fault step of 3–4 km, greater than which earthquake ruptures would not propagate (Wesnousky 2006), if the difference in slip sense were ignored. However, broadening a fault zone due to such a bifurcation to the surface will probably lead to widening of the areas affected by strong ground motion.

Conclusion

Geologic observations of the surface rupture associated with the Mw = 7.0 16 April Kumamoto earthquake revealed ~10-km stretch of two parallel rupture strands of strike-slip and normal fault reoccupying older fault scarps along the Futagawa and Idenokuchi faults, respectively. The locations and slip motions of the rupture zones were also manifested as interferogram fringe offsets in InSAR images. Coupled with the aftershock distribution, seismic and geodetic inversions from other studies, we found that slip-partitioned fault breaks occurred during the Kumamoto earthquake under a complex stress field, leading to oblique fault motion mixed with right-lateral shear and extension on the southern margin of the Beppu-Shimabara Rift Zone (BSRZ). The Kumamoto rupture is the second significant case of coseismic slip partitioning. Our simple dislocation model with a subsurface oblique-slip fault demonstrates that such a bifurcation into pure strike-slip and normal faults likely occurs near the surface for optimally oriented failure. This provides an insight into scale- and depth-dependent stress heterogeneity. In seismic hazard estimates, the Kumamoto case also provides an implication to estimate a single seismic source fault in multiple fault strands regardless of slip sense, which may influence the estimated size of the strong shaking areas.

Authors' contributions

ST organized the field survey in the study area, conducted the modeling and drafted the manuscript. ST, HK, SO, DI, and ZM mapped the surface rupture and measured fault slip in the field. ZM contributed to revise English sentences. All authors have read and approved the final manuscript.

Author details

[1] International Research Institute of Disaster Science, Tohoku University, Aoba, 468-1, Aoba, Sendai 980-0845, Japan. [2] Department of Earth Sciences, Chiba University, Yayoi-cho 1-33, Inage-ku, Chiba 263-8522, Japan. [3] Department of Geography, Tokyo Metropolitan University, Minami-osawa 1-1, Hachioji, Tokyo 192-0397, Japan. [4] Institute for Risk and Disaster Reduction, University College London, Gower Street, London WC1E 6BT, UK.

Acknowledgements

We acknowledge the helpful discussions and interactions in the field with Yasuhiro Kumahara and the other members of the 2016 Kumamoto earthquake surface rupture mapping group. We also thank Naoya Takahashi, Tomoki Tanaka and Shintaro Kashihara for their support during our field mapping. Our field work was supported by Tohoku University and The Ministry of Education, Culture, Sports, Science and Technology (MEXT) KAKENHI Grant Numbers 16H06298 and 16H03112. Travel expenses for ZM were provided by the Short-Term Fellowship program (No. PE15776), Japan Society for the Promotion of Science (JSPS).

Competing interests

The authors declare that they have no competing interests.

Received: 15 July 2016 Accepted: 29 October 2016
Published online: 22 November 2016

References

Bowman D, King G, Tapponnier P (2003) Slip partitioning by elastoplastic propagation of oblique slip at depth. Science 300:1121–1123

Fitch T (1972) Plate convergence, transcurrent faults, and internal deformation adjacent to southeast Asia and the western Pacific. J Geophys Res 77:4432–4462

Geospatial Information Authority of Japan (2016a) The 2016 Kumamoto Earthquake: Crustal deformation around the faults (in Japanese). http://www.gsi.go.jp/BOUSAI/H27-kumamoto-earthquake-index.html#3. Accessed 25 June 2016

Geospatial Information Authority of Japan (2016b) The 2016 Kumamoto Earthquake: Crustal deformation around the faults (in Japanese), postseismic deformation. http://www.gsi.go.jp/common/000140323.png Accessed 25 June 2016

Ishizaka S, Iwasaki Y, Hase Y, Watanabe K, Iwauchi A, Taziri M (1995) Subsidence rate and sediments of the last interglacial epoch in the Kumamoto Plain, Japan. Quat Res 34:335–344 **(in Japanese with English abstract)**

Jones CH, Wesnousky SG (1992) Variations in strength and slip rate along the San Andreas fault system. Science 256:83–86

Kamata H, Kodama K (1994) Tectonics of an arc-arc junction: an example from Kyushu Island at the junction of the Southwest Japan Arc and the Ryuku Arc. Tectonophysics 233:69–81

Kamata H, Uto K, Uchiumi S (1988) Geochronology and evolution of the post-Shishimuta caldera activity around the Waitasan area in the Hohi volcanic zone, Kyushu, Japan. Bull Volcanol Soc Jpn 33:305–320

King G, Klinger Y, Bowman D, Tapponnier P (2005) Slip-partitioned surface breaks for the Mw 7.8 2001 Kokoxili earthquake, China. Bull Seismol Soc Am 95:731–738

Kubo H, Suzuki W, Aoi S, Sekiguchi H (2016) Source rupture processes of the 2016 Kumamoto, Japan, earthquakes estimated from strong-motion waveforms. Earth Planets Space 68:161–173. doi:10.1186/s40623-016-0536-8

Kumahara Y, Goto H, Nakata T, Ishiguro S, Ishimura D, Ishiyama T, Okada S, Kagohara K, Kashihara S, Kaneda H, Sugito N, Suzuki Y, Takenami T, Tanaka K, Tanaka T, Tsutsumi H, Toda S, Hirouchi D, Matsuta N, Mita T, Moriki H, Yoshida H, Watanabe M (2016) Distribution of surface rupture associated the 2016 Kumamoto earthquake and its significance. Abstract (MIS34-05)

of the Japan Geoscience Union Meeting 2016. http://www2.jpgu.org/meeting/2016/PDF2016/M-IS34_O.pdf Accessed 25 June 2016
Kumamoto Prefecture (1996) Survey report on the Futagawa and Tatsutayama faults. http://www.hp1039.jishin.go.jp/danso/Kumamoto2Afrm.htm Accessed 12 July 2016 **(in Japanese)**
Matsumoto Y (1979) Some problems on volcanic activities and depression structures in Kyushu, Japan. Mem Geol Soc Jpn 16:127–139
McCaffrey R (1992) Oblique plate convergence, slip vectors, and forearc deformation. J Geophys Res 97:8905–8915
Michael A (1984) Determination of stress from slip data: faults and folds. J Geophys Res 89:11517–11526
Nakata T, Imaizumi T (eds) (2002) Digital active fault map of Japan. University of Tokyo Press, Tokyo DVD
Nishimura S, Hashimoto M (2006) A model with rigid rotations and slip deficits for the GPS-derived velocity field in southwest Japan. Tectonophysics 421:187–202
Okada Y (1992) Internal deformation due to shear and tensile faults in a half-space. Bull Seismol Soc Am 82:1018–1040
Ono K, Watanabe K (1985) Geological map of Aso Volcano. In: Geological Map of Volcanoes. No. 4 Geological Survey of Japan
Research Group for Active Faults of Japan (1991) Active Faults in Japan, sheet maps and inventories, rev. ed. Univ of Tokyo Press, Tokyo
Research Group for Active Tectonics in Kyushu (1989) Active Tectonics in Kyushu, Univ. of Tokyo Press, Tokyo
Sibson RH (1992) Implications of fault-valve behavior for rupture nucleation and recurrence. Tectonophysics 211:283–293
Smith DE, Heaton TH (2011) Models of stochastic, spatially varying stress in the crust compatible with focal-mechanism data, and how stress inversions can be biased toward the stress rate. Bull Seismol Soc Am 101:1396–1421
Tada T (1984) Spreading of the Okinawa Trough and its relation to the crustal deformation in the Kyushu. J Seismol Soc Jpn 37:407–415
Tsukuda E (1990) Active tectonics of the median tectonic line. Bull Geol Surv Jpn 41:405–406 **(in Japanese)**
Watanabe K, Momikura Y, Tsuruta K (1979) Active faults and parasitic eruption centers on the western flank of Aso Caldera, Japan. Quat Res 18:89–101 **(in Japanese with English abstract)**
Wesnousky SG (2006) Predicting the endpoints of earthquake ruptures. Nature 444:358–360. doi:10.1038/nature05275
Yabe H (1925) The "Nagasaki Dreiecke" proposed by Prof. Richthofen ("Richthofen-shi no Nagasaki-sankaku-chiiki" in Japanese). J Geol Soc Jpn 32:201–209 **(in Japanese)**